Electronic Supplementary Material (ESI) for Inorganic Chemistry Frontiers.

Supplemental Information

Interface Engineering of CoS/MoS_2 Heterostructure for Electrocatalytic Reduction of N_2 to NH_3

Yixian Liu,†[a,b] Ruqiang Wu,†[a] Yunliang Liu,[a] Peiji Deng,[a] Yaxi Li,[a] Yuanyuan Cheng,[a] Yongchao Du,[a] Zenan Li,[c] Xiong Yan,[c] Naiyun. Liu,*[a] Zhenhui Kang,*[c,d] and Haitao Li*[a]

a. Institute for Energy Research, School of Chemistry and Chemical Engineering, Jiangsu University, Zhenjiang, 212013, Jiangsu, China. E-mail: liuny@ujs.edu.cn, zhkang@suda.edu.cn, liht@ujs.edu.cn.
b. China National Textile and Apparel Council Key Laboratory of Flexible Devices for Intelligent Textile and Apparel, Soochow University, Suzhou 215123, China.
c. Institute of Functional Nano & Soft Materials (FUNSOM), Jiangsu Key Laboratory for Carbon-Based Functional Materials & Devices, Soochow University, Suzhou, 215123, Jiangsu, China.
d. Macao Institute of Materials Science and Engineering (MIMSE), MUST−SUDA Joint Research Center for Advanced Functional Materials, Macau University of Science and Technology, Taipa 999078, Macao, China.

Appendix A: The transient photovoltage (TPV) measurements

TPV measurement is based on stimuli-response method, which can be carried out at room temperature on a self-made platform. In the platform, the platinum wire is used as the counter electrode, and the working electrode is made by ITO with dried solution (200μl, by dispersing 10mg sample uniformly in 2ml ethanol and then applied an ultrasonic treatment). As shown in Fig. S0, the sample was excited by the third-harmonic Nd: YAG laser (Laser beam with a wavelength of 355nm, pulse width of 5ns and excitation frequency 5Hz. Polaris II, New Wave Research, Inc.). The feedback signal was amplified by 50 times in a signal amplifier, recorded by the digital oscilloscope and the signal acquisition card.

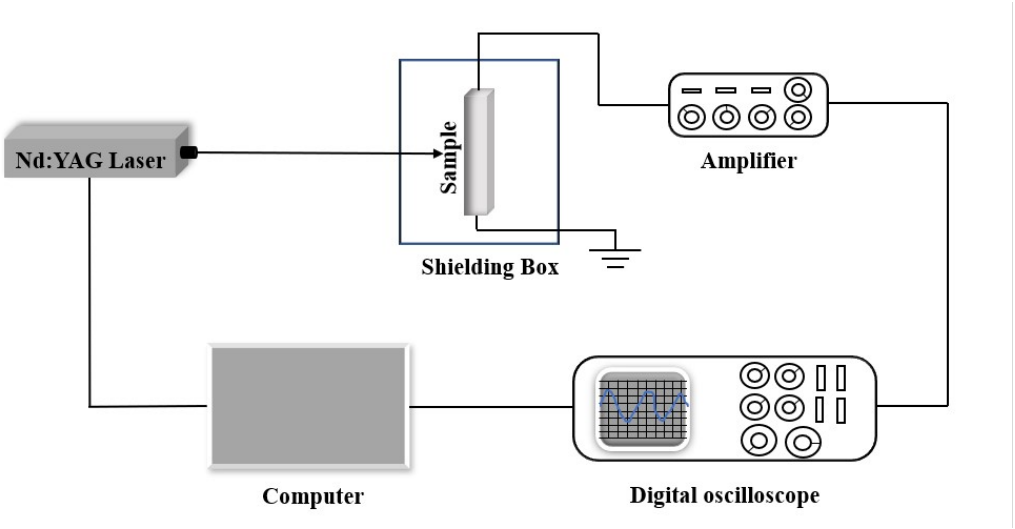

Figure S0. Schematic diagram of Transient photovoltage test system.[1]

Appendix B: CoS/MoS_2 synthesized in solutions with different Mo/Co ratio

The material shown in paper is synthesized from a precursor solution whose ratio of Co to Mo is 1:5. We also prepared samples by heating solution with ratio of Co to Mo being 1:4 and 1:6 to investigate the effect of concentration on structure of final product.

The preparation process of precursor solution with different ratio of Co and Mo is as same as that of shown in paper, except that the mass of $CoCl_2 \cdot 6H_2O$ (29.7 mg in paper) and CH_4N_2S (23.8 mg in paper) added into ethylene glycol solution were adjusted to 37.2 mg and 29.8 mg to achieve Co: Mo = 1:4 in one product solution. For preparing another solution with different ratio of Co to Mo (1:6), the added $CoCl_2 \cdot 6H_2O$ and CH_4N_2S are 24.8 mg and 19.9 mg, respectively. The mass of MoS_2 powder remain unchanged.

The TEM images and element mapping results are shown in Fig. S1. As shown in Fig. S1a and b, both MoS_2 and CoS can be found in the structure, regardless of the concentration of precursor solution adopted in the present work. According to the element mappings (Fig.S1c-g) and elements ratio analysis, there's no significant difference in loading of CoS with the change of ratio of Co: Mo, and in all of the samples prepared in the present work, the quantity of loaded CoS is bare, since the signals of Co are weak in all of the studied samples.

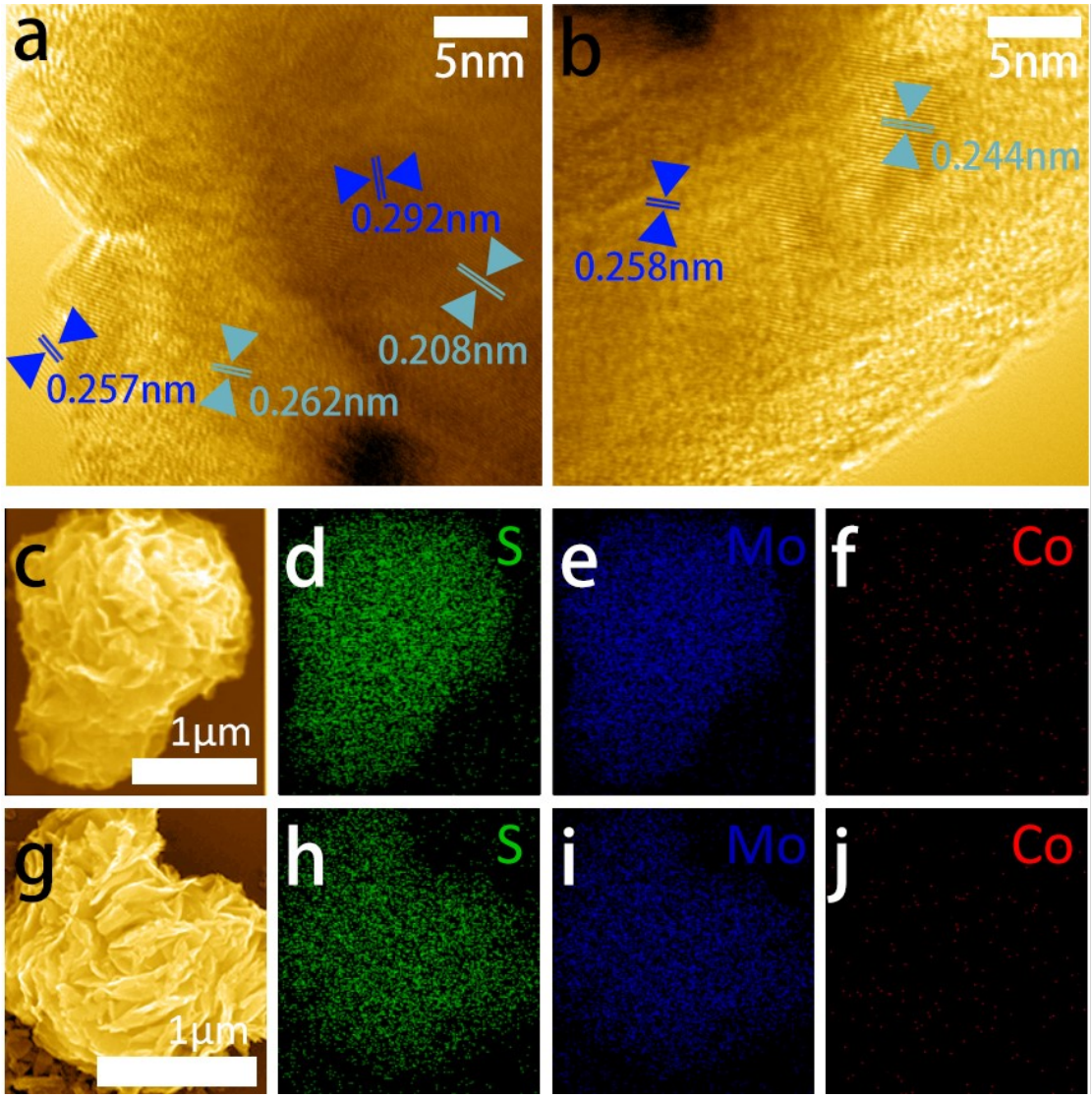

Figure S1. The TEM images of CoS/MoS_2 synthesized in solution whose ratio of Co to Mo are (a) 1:4 and (b) 1:6, respectively, and the SEM image of CoS/MoS_2 synthesized in solution with (c) Co: Mo = 1: 4 and (g) Co: Mo = 1: 6. The element mapping of (d) S, (e) Mo and (f) Co are associated to the particles in (c), while the element mapping of (h) S, (i) Mo and (j) Co are associated to the particles in (g). The plane in TEM image (a) and (b) cited by dark blue belongs to CoS, while the ones cited by blue-gray are MoS_2. In TEM image (a), the (100) and (101) plane of CoS can be observed clearly, while (101) and (103) plane of MoS_2 are observed. In TEM image (b), (101) of CoS and (102) of MoS_2 are observed.

Appendix C: Other supplemental figures

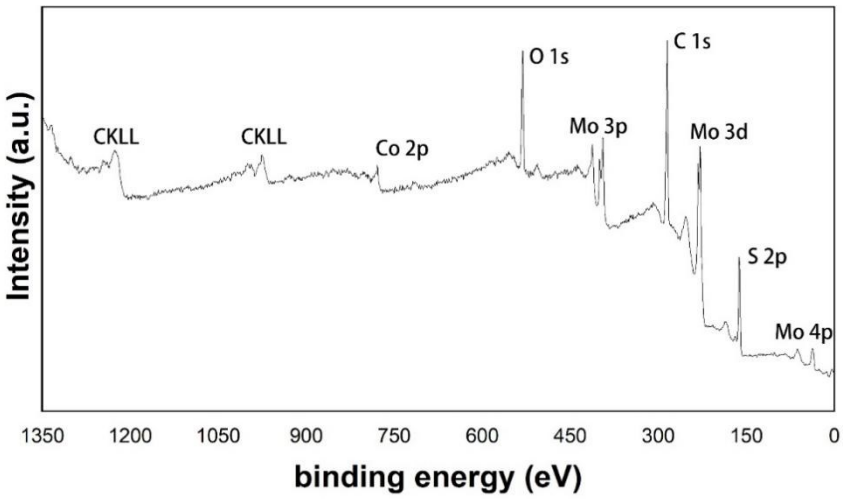

Figure S2. XPS survey spectrum of CoS/MoS_2.

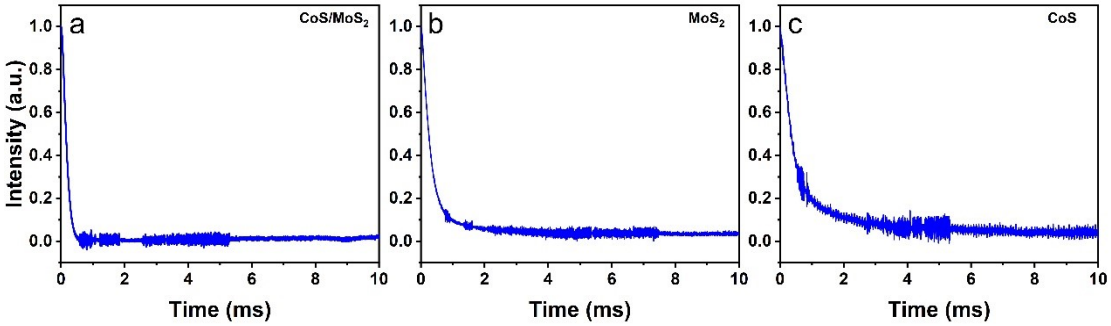

Figure S3. Original TPV data of (a)CoS/MoS_2, (b)MoS and (c)CoS.

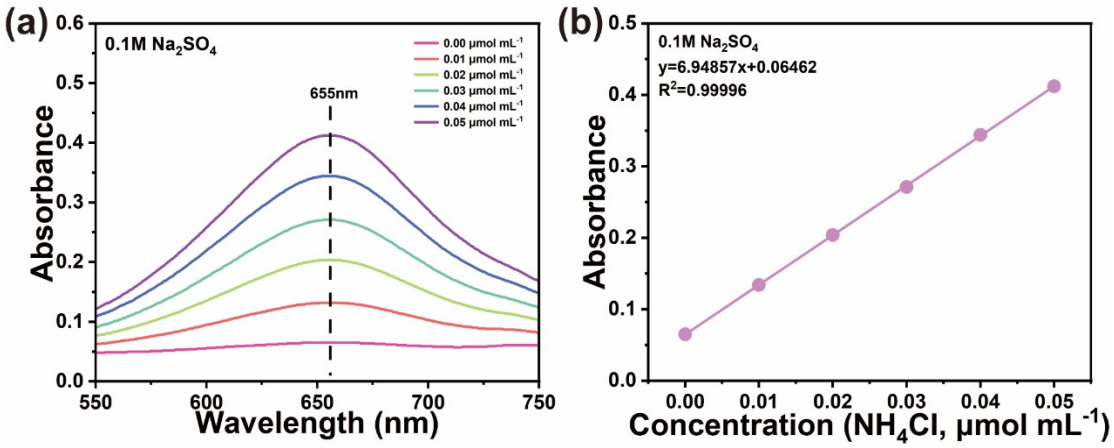

Figure S4. (a)Ultraviolet absorption spectra and (b) concentration-absorbance linear relationship for indophenol blue method.

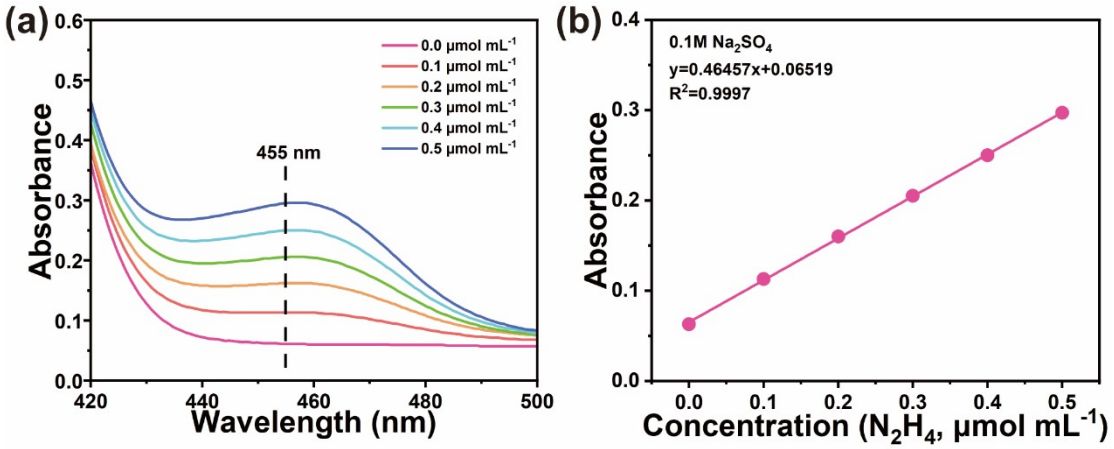

Figure S5. (a)Ultraviolet absorption spectra and (b) concentration-absorbance linear relationship for Watt and Chrisp method.

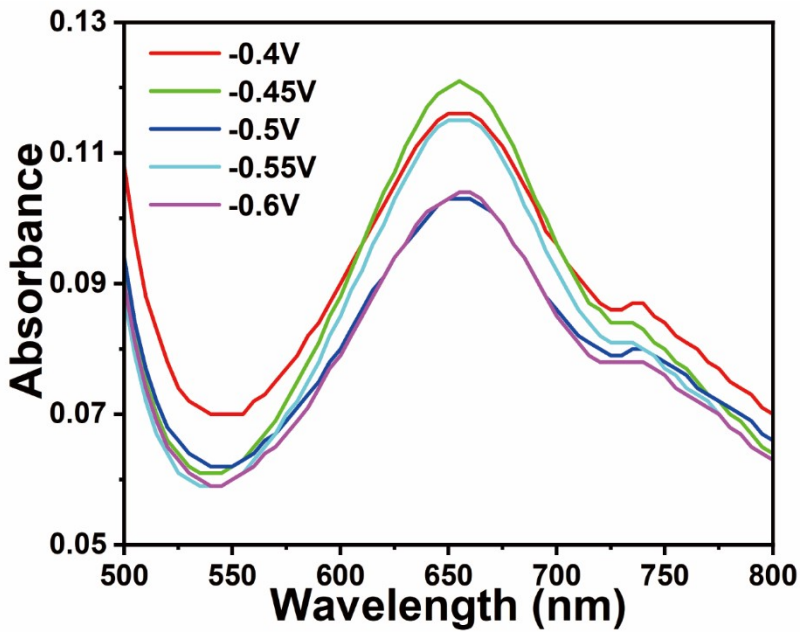

Figure S6. (a) Ultraviolet absorption spectra of after-reaction N_2-saturated solution under different potentials.

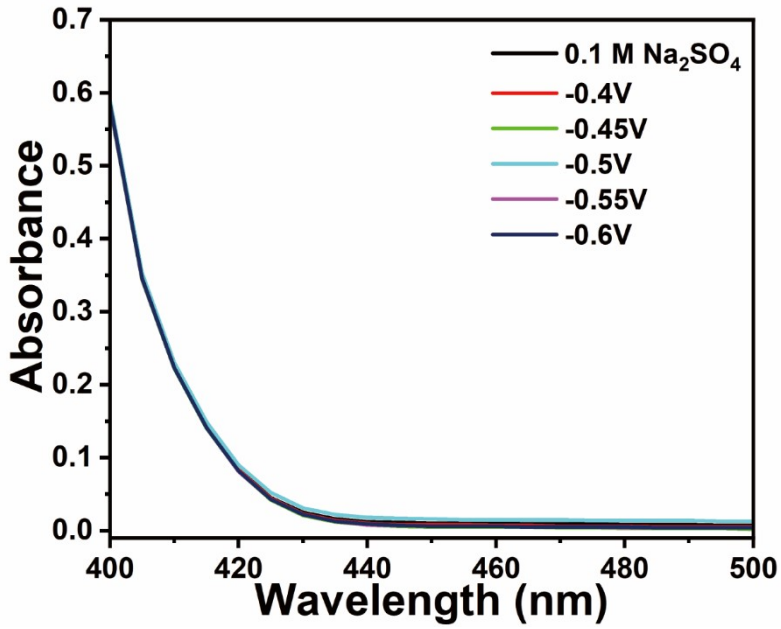

Figure S7. (a)Ultraviolet absorption spectra of after-reaction N_2-saturated solution under different potentials.

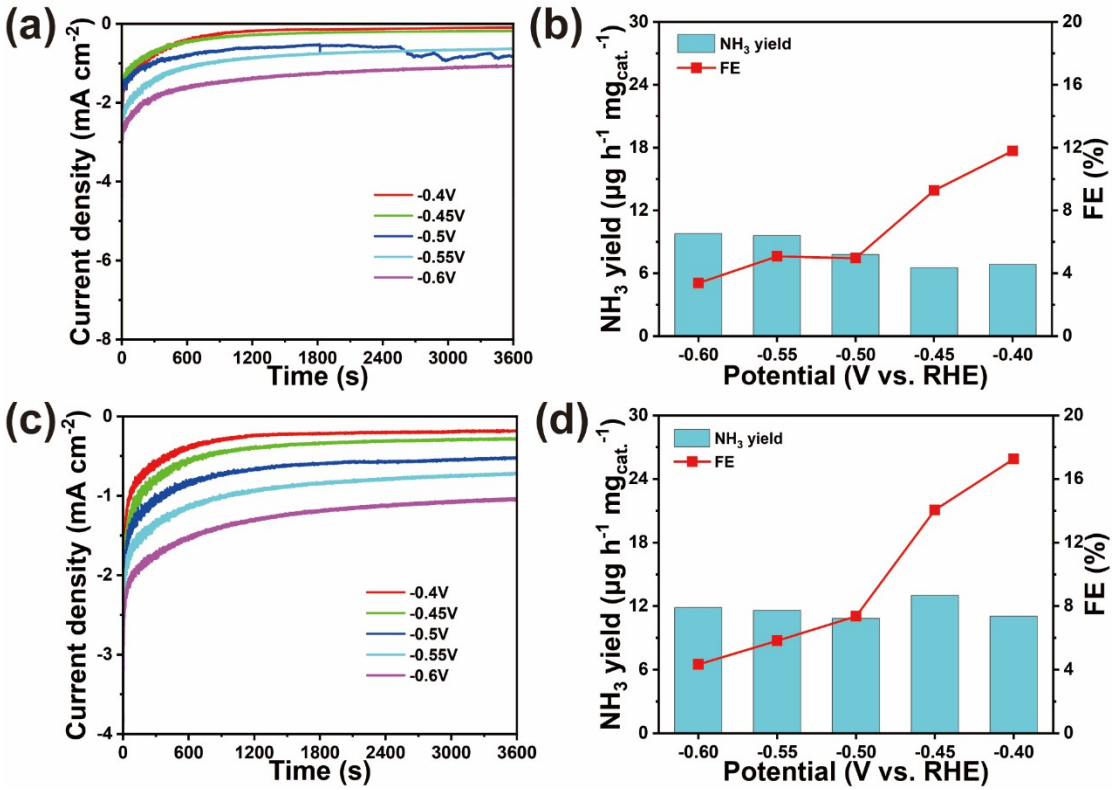

Figure S8. I-T curves of (a) MoS_2 and (c) CoS, and ammonia yields and FEs of (b) MoS_2 and (d) CoS.

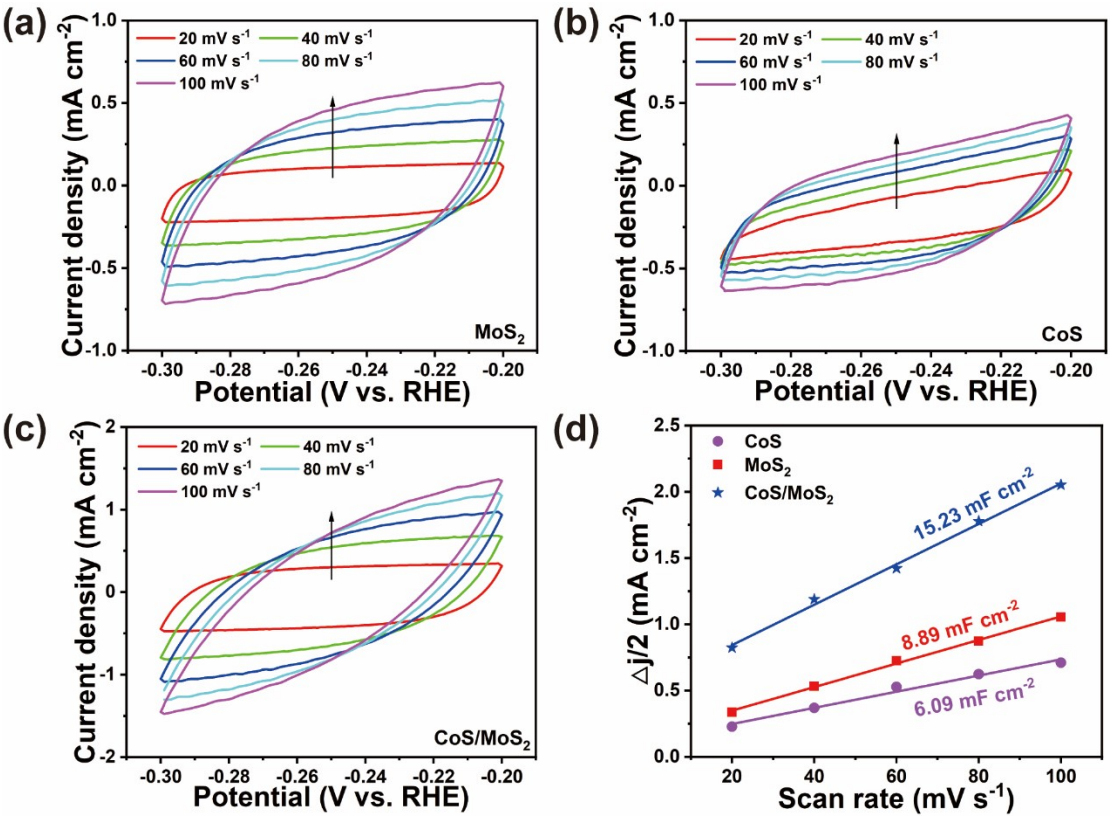

Figure S9. Cyclic voltammetry (CV) of (a) MoS_2, (b) CoS and (c) CoS/MoS_2, and (d) the derived double-layer capacitance.

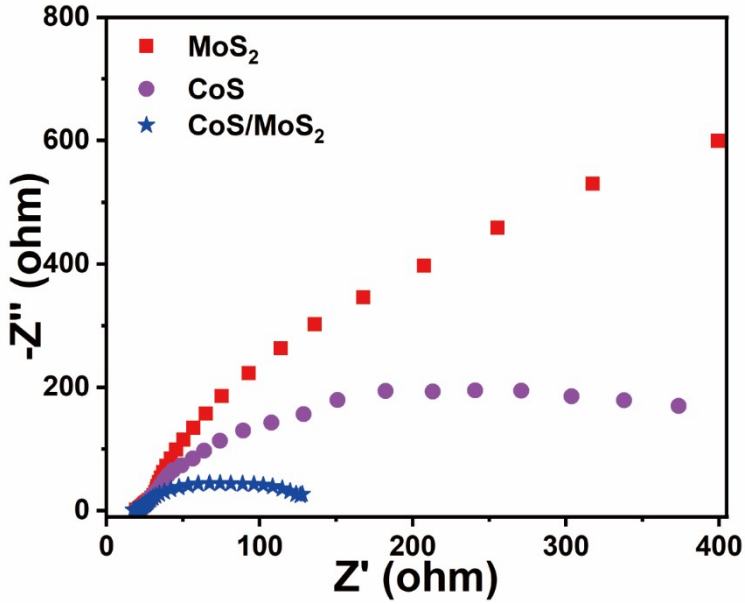

Figure S10. EIS of MoS_2, CoS and CoS/ MoS_2.

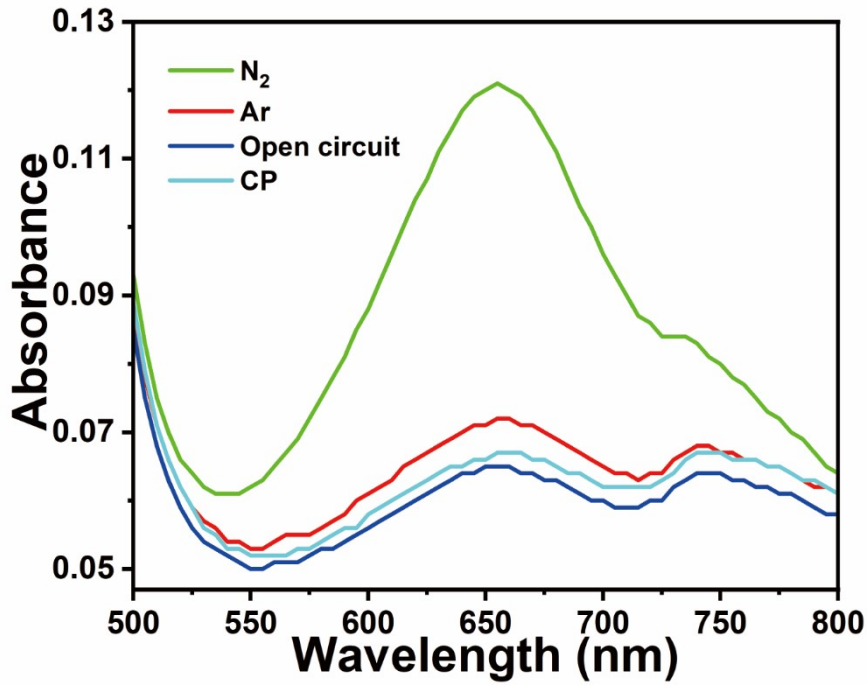

Figure S11. The UV-vis adsorption spectra of CoS/MoS_2 electrode in N_2-saturated solution for 1 hr at -0.45 V vs. RHE, CoS/MoS_2 electrode in Ar-saturated solution for 1 hr at -0.45 V vs. RHE, bare carbon caper electrode in N_2-saturated solution for 1 hr at -0.45 V vs. RHE, and the CoS/MoS_2 electrode in N_2-saturated solution for 1 hr at open circuit potential.

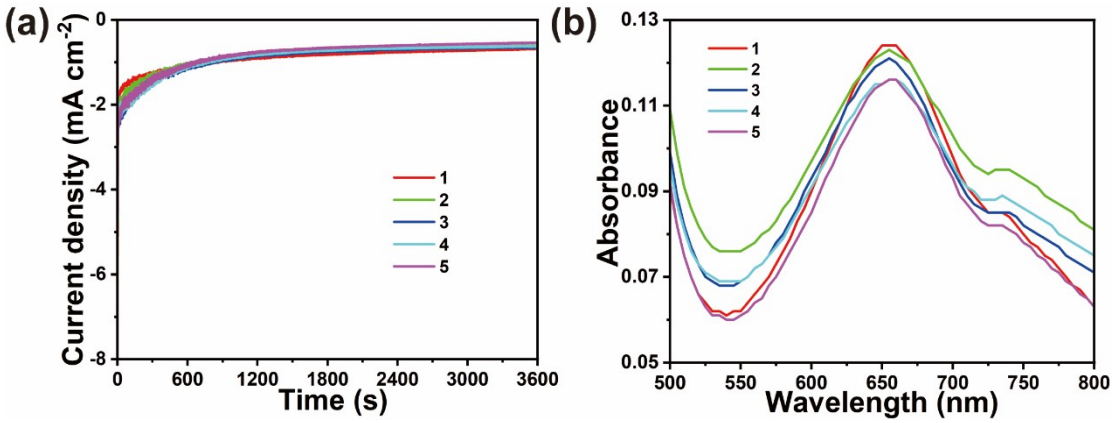

Figure S12. (a) The I-T curves of five cycles and the (b) corresponding UV-vis adsorption spectra.

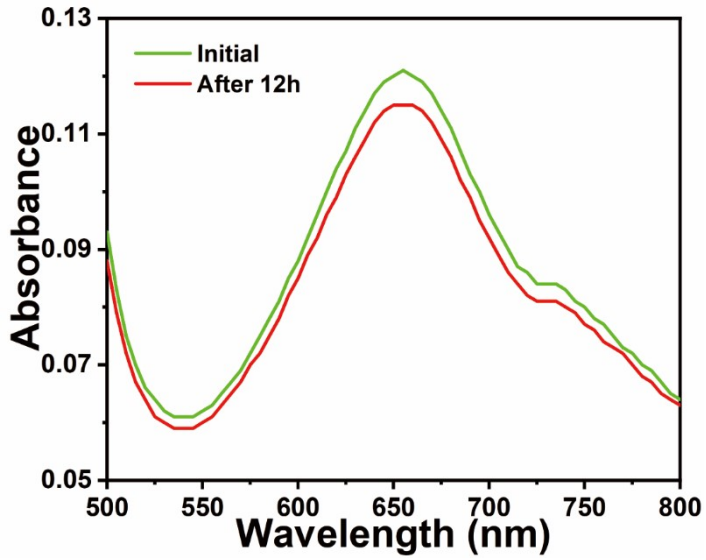

Figure S13. The UV-vis adsorption of two 1-hr-tests before and after 12-hr-chronoamperometric test.

Table S1. Some reported electrocatalysts for NRR

Catalyst	Yield rate of NH_3	FE (%)	Electrode	Reference
Vo-MoO_2@C	9.75 μg h^{-1} $mg_{cat.}^{-1}$	3.24	0.1M Na_2SO_4	[2]
Fe-MoS_2	8.63 μg h^{-1} $mg_{cat.}^{-1}$	18.8	0.5 M K_2SO_4	[3]
Mo_2C/NC	70.6 μmol h^{-1} $g_{cat.}^{-1}$	12.3	0.1M Na_2SO_4	[4]
Mo-Co/NC	89.8 μmol h^{-1} $mg_{cat.}^{-1}$	13.5	0.1M Na_2SO_4	[5]
MoN NA/CC	3.01×10^{-10} mo1 s^{-1} cm^{-2}	1.15	0.1M HCl	[6]
MoO_3 nanosheet	4.80×10^{-10} mol s^{-1} cm^{-2}	1.9	0.1M HCl	[7]
NiO-NF-3.0	16.16 μg h^{-1} $mg_{cat.}^{-1}$	9.17	0.1M Na_2SO_4	[8]
NiFe-nanomesh array	16.89 μg h^{-1} $mg_{cat.}^{-1}$	12.5	0.1M Na_2SO_4	[9]
Fe/Fe_3O_4	0.19 μg h^{-1} cm^{-2}	8.29	0.1M PBS	[10]
5%Fe-$NiMoO_4$	15.36 μg h^{-1} $mg_{cat.}^{-1}$	26.85	0.1M Na_2SO_4	This work

Reference

1. Y. Li, Y. Liu, X. Liu, Y. Liu, Y. Cheng, P. Zhang, P. Deng, J. Deng, Z. Kang and H. Li, Fe-doped SnO_2 nanosheet for ambient electrocatalytic nitrogen reduction reaction, *Nano Research*, 2022, **15**, 6026-6035.
2. Y. Du, Z. He, F. Ma, Y. Jiang, J. Wan, G. Wu and Y. Liu, Anionic Biopolymer Assisted

Preparation of MoO_2@C Heterostructure Nanoparticles with Oxygen Vacancies for Ambient Electrocatalytic Ammonia Synthesis, *Inorganic Chemistry*, 2021, **60**, 4116-4123.

3. H. Su, L. Chen, Y. Chen, R. Si, Y. Wu, X. Wu, Z. Geng, W. Zhang and J. Zeng, Single Atoms of Iron on MoS_2 Nanosheets for N_2 Electroreduction into Ammonia, *Angewandte Chemie International Edition*, 2020, **59**, 20411-20416.
4. Y. Zhang, J. Hu, C. Zhang, A. T. F. Cheung, Y. Zhang, L. Liu and M. K. H. Leung, Mo_2C Embedded on Nitrogen-doped Carbon toward Electrocatalytic Nitrogen Reduction to Ammonia under Ambient Conditions, *Int. J. Hydrogen Energy*, 2021, **46**, 13011-13019.
5. Y. Zhang, J. Hu, C. Zhang, Y. Liu, M. Xu, Y. Xue, L. Liu and M. K. H. Leung, Bimetallic Mo-Co Nanoparticles Anchored on Nitrogen-doped Carbon for Enhanced Electrochemical Nitrogen Fixation, *J. Mater. Chem. A*, 2020, **8**, 9091-9098.
6. L. Zhang, X. Ji, X. Ren, Y. Luo, X. Shi, A. M. Asiri, B. Zheng and X. Sun, Efficient Electrochemical N_2 Reduction to NH_3 on MoN Nanosheets Array under Ambient Conditions, *ACS Sustainable Chem. Eng.*, 2018, **6**, 9550-9554.
7. J. Han, X. Ji, X. Ren, G. Cui, L. Li, F. Xie, H. Wang, B. Li and X. Sun, MoO_3 Nanosheets for Efficient Electrocatalytic N_2 Fixation to NH_3, *J. Mater. Chem. A*, 2018, **6**, 12974-12977.
8. M. Zhou, W. Xiong, H. Li, D. Zhang and Y. Lv, Emulsion-template Synthesis of Mesoporous Nickel Oxide Nanoflowers Composed of Crossed Nanosheets for Effective Nitrogen Reduction, *Dalton Trans.*, 2021, **50**, 5835-5844.
9. Y. Sun, T. Jiang, J. Duan, L. Jiang, X. Hu, H. Zhao, J. Zhu, S. Chen and X. Wang, Two-Dimensional Nanomesh Arrays as Bifunctional Catalysts for N_2 Electrolysis, *ACS Catal.*, 2020, **10**, 11371-11379.
10. L. Hu, A. Khaniya, J. Wang, G. Chen, W. E. Kaden and X. Feng, Ambient Electrochemical Ammonia Synthesis with High Selectivity on Fe/Fe Oxide Catalyst, *ACS Catal.*, 2018, **8**, 9312-9319.